Kauppinen, Christoffer; Isakov, Kirill; Sopanen, Markku

# Grass-like Alumina with Low Refractive Index for Scalable, Broadband, Omnidirectional Antireflection Coatings on Glass Using Atomic Layer Deposition

*Published in:*
ACS Applied Materials and Interfaces

*DOI:*
10.1021/acsami.7b01733

Published: 11/04/2017

*Document Version*
Publisher's PDF, also known as Version of record



*Please cite the original version:*
Kauppinen, C., Isakov, K., & Sopanen, M. (2017). Grass-like Alumina with Low Refractive Index for Scalable, Broadband, Omnidirectional Antireflection Coatings on Glass Using Atomic Layer Deposition. *ACS Applied Materials and Interfaces*, *9*(17), 15038−15043. https://doi.org/10.1021/acsami.7b01733

ACS AUTHORCHOICE

ACS APPLIED MATERIALS & INTERFACES

Research Article

www.acsami.org

# Grass-like Alumina with Low Refractive Index for Scalable, Broadband, Omnidirectional Antireflection Coatings on Glass Using Atomic Layer Deposition

Christoffer Kauppinen,[*,†,‡] Kirill Isakov,[†,‡] and Markku Sopanen[†]

[†]Department of Micro- and Nanosciences, Micronova, Aalto University, P.O. Box 13500, FI-00076 Aalto, Finland

**ABSTRACT:** We present a new type of nanoporous antireflection (AR) coating based on grass-like alumina with a graded refractive index profile. The grass-like alumina AR coating is fabricated using atomic layer deposition (ALD) of alumina and immersion in heated deionized water. Optical transmittance of 99.5% at 500 nm was achieved with average transmittance of 99.0% in the range of 350−800 nm at normal incidence for double-sided coated glass. Angular spectral transmittance (0−80°) of the double-sided AR coated glass was also measured in the range of 350−800 nm and found to have mean spectral transmittance of 94.0% at 60°, 85.0% at 70°, and 53.1% at 80° angles of incidence, respectively. The grass-like alumina AR coating is suitable for mass production with the presented technique: even hundreds of optical components can be coated in parallel. Furthermore, as an ALD-based technique, the coating can be deposited conformally on surfaces with extreme topography, unlike many spin-coating, physical vapor deposition or glancing angle deposition-based coatings used today.

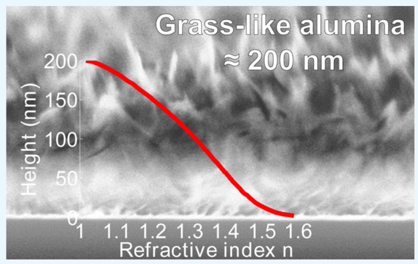


**KEYWORDS:** *ALD, atomic layer deposition, alumina, antireflection, graded index, broadband, omnidirectional, nanoporous*



## 1. INTRODUCTION

Antireflection (AR) coatings are perhaps the most universal feature in all of optics, as they are used everywhere from camera lenses to high-performance solar cells. Typically, AR coatings seek to minimize reflection by texturing the original surface[1] or by coating the surface with a suitable dielectric material. With a single AR layer, the Fresnel reflection at normal incidence is minimized when the refractive index of the AR layer is $n_{AR} = \sqrt{n_{substrate} n_{air}}$, and the optical thickness of the layer is chosen to be a quarter of the wavelength. This means that glass, the most widely used optical material, with refractive index of approximately 1.5 should have an AR coating with refractive index of 1.22. This is problematic as $MgF_2$, the lowest refractive index inorganic material, has a refractive index of 1.38.[2]

Introducing nanoscale porosity into materials is a way to artificially lower the effective refractive index of the material. The increased porosity lowers the density, thus lowering the effective refractive index. Nanoporous materials have been studied vigorously as AR coatings for glass and other materials.[2−11] Often nanoporous AR coatings are manufactured with a gradient refractive index profile[5−10] due to the well-known broadband and omnidirectional AR properties a gradient-index layer provides.[12,13] In addition to nanoporous AR coatings, there has been intense research in optical reflectionless potentials and reflection suppressing metamaterials in recent years.[14,15] The most common deposition methods for nanoporous AR coatings are spin-coating[3,9] and glancing angle deposition.[4−6,8,10,11] Neither of these techniques scales well to coating hundreds or thousands of components in parallel, nor do they permit coating all the surfaces of an object with a single run, though the obtained performances are excellent.

Chemical instability of alumina films made by atomic layer deposition (ALD) in heated water has been well-established,[16,17] as have the morphology changes during long-term exposure to water.[18,19] In this study, we exploited this morphology change by using short-term (30 min) immersion of ALD alumina films to heated (20−90 °C) deionized water (DIW) to study the formation of grass-like alumina and its AR properties on glass. This grass-like alumina is extremely interesting as a nanoporous AR coating due to its scalability, ability to coat all surfaces with one run, excellent optical transmittance, and gradient refractive index, but has not so far been used in this capacity, although porous anodic alumina and sol−gel-based aluminas (some with "flower-like" structures using the hot water treatment) have been.[2,20−25] Neither porous anodic alumina nor sol−gel-based aluminas produce conformal coatings,[26] and the presented grass-like alumina AR coating is the first conformal nanoporous AR coating made from alumina and the first nanoporous AR coating made using DIW immersion of ALD alumina.

## 2. EXPERIMENTAL SECTION

The amorphous ALD alumina was deposited on Corning microscope slides ($n$ = 1.48, from Brewster's angle) with a BENEQ TFS500 ALD reactor using the classic water−trimethylaluminum (TMA) process[27] at a reactor temperature of 120 °C and pressure of 5 mbar. The

**Received:** February 6, 2017
**Accepted:** April 11, 2017
**Published:** April 11, 2017

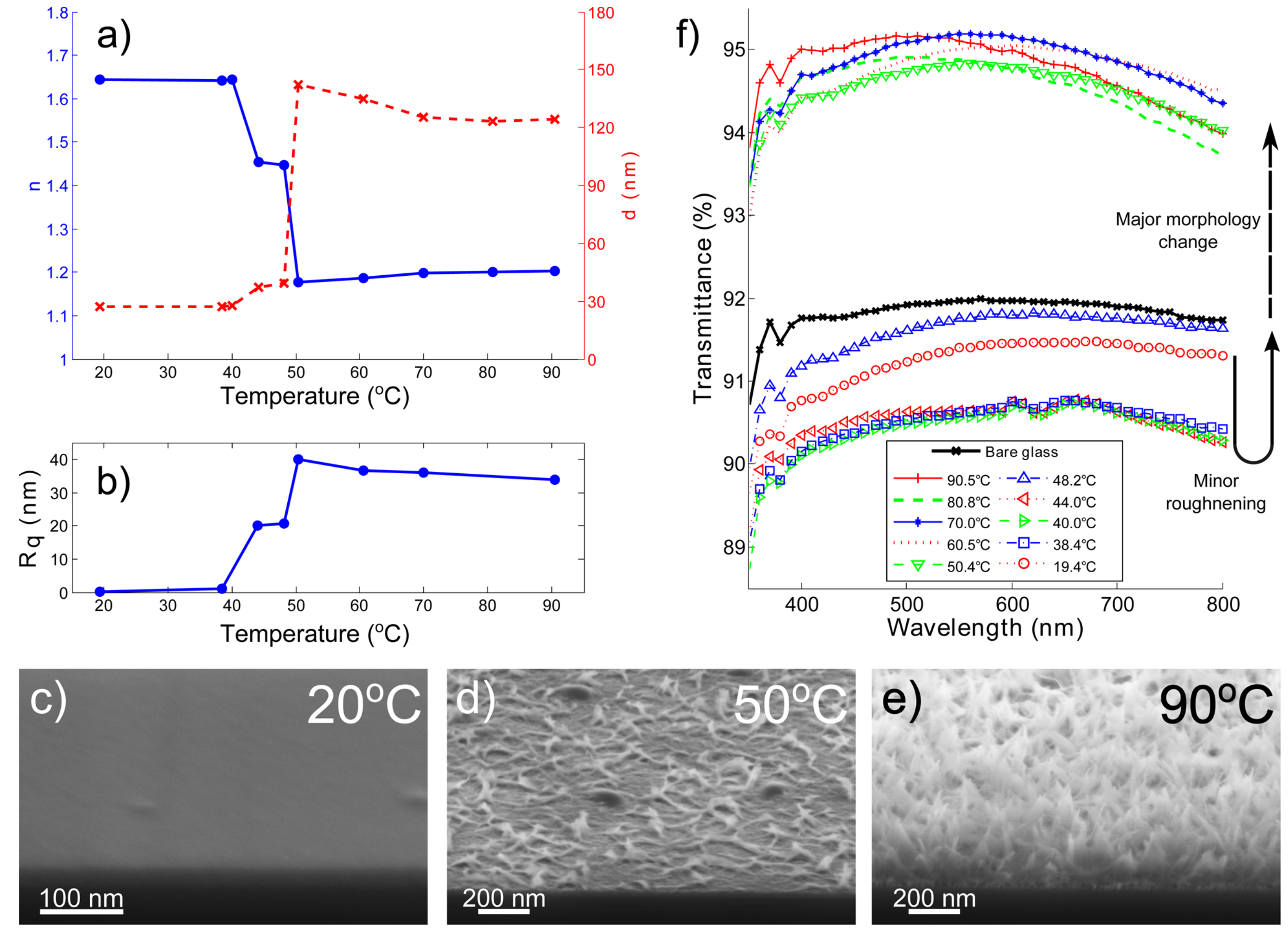


**Figure 1.** (a) Refractive index and thickness of the treated alumina films as a function of the DIW treatment temperature measured using ellipsometry from the silicon samples. The dots mark the measured refractive indices, and the crosses mark the thicknesses. (b) AFM measurements of the surface roughness from the silicon samples. The horizontal axes are identical in panels a and b. (c−e) SEM images of the ALD alumina processed at different DIW temperatures. The imaging angle was 18° from the plane of the surface. (f) Transmission spectra of single-sided coated glass samples at normal incidence. The solid arrow shows the trend of the transmittance as the DIW temperature is increased toward 50 °C. The dashed arrow shows the dramatic increase in transmittance with temperatures over 50 °C.

number of cycles was 313; the TMA pulse time was 200 ms, and the purge time for TMA was 1.9 s. The water pulse time was 200 ms; the purge for water was 2.15 s, and for the carrier gas (nitrogen), the flow was 200 sccm. In addition to these, a constant nitrogen flow of 150 sccm was let into the reactor throughout the deposition. This process resulted in 28 nm-thick ($n$ = 1.64) uniform alumina layer on a silicon wafer. The alumina layer was grown on a Si wafer with natural oxide on the surface (due to atmospheric oxygen) and on all measured glass slides excluding reference glass slides. As the surface of the silicon wafer was oxidized before ALD, we presume that the growth conditions for the alumina on the oxidized silicon surface are closely similar to the growth conditions of alumina on glass and that the deposited thicknesses are the same. Pieces of the ALD alumina coated silicon wafer were each paired with a similarly coated glass slide and processed together, ensuring identical treatments. This pairing was done to measure the refractive index and thickness of the coating from the silicon sample using ellipsometry (Plasmos He−Ne ellipsometer) before and after DIW treatment, as the measurement is very difficult from transparent glass slides. Two series of samples were made: single-sided coated samples and double-sided coated samples. Both series were processed in a beaker of DIW inside an IKA HBR 4 digital heat bath with built-in temperature control. In both series, the temperature was first stabilized before inserting the sample to accurately know the water temperature. Optical transmittance of 99.5% at 500 nm was achieved as well as average transmittance of 99.0% over the range of 350−800 nm at normal incidence. Angular spectral transmittance (0−80°) of the double-sided AR coated glass was also measured in the range of 350−800 nm and found to have mean spectral transmittance of 94.0% at 60°, 85.0% at 70°, and 53.1% at 80° angles of incidence, respectively. All transmittances in this paper were measured using an Agilent Cary 7000 Universal Measurement spectrophotometer. Suitability of the grass-like alumina coating for surfaces with extreme topography was studied by conformally coating black silicon surfaces with grass-like alumina and taking cross section scanning electron microscope (SEM) images. The black silicon was fabricated with cryogenic inductively coupled reactive ion etching using common parameters found in literature.[28−30]

## 3. RESULTS AND DISCUSSION

Figure 1a shows the effect of different DIW treatment temperatures on the film thickness and refractive index (both from ellipsometry), while Figure 1b shows how the DIW temperature affects the root-mean-square surface roughness ($R_q$) measured using AFM. The changes were so large that we repeated the deposition with another BENEQ TFS500 reactor with similar results. It can be seen from Figures 1a and b that the alumina film shows negligible change below 40 °C; between 40 and 50 °C, some roughening occurs and the thickness increases, and above 50 °C, a dramatic change in the film occurs. The dramatic increase in surface roughness happens simultaneously with the sharp decrease in refractive index and the jump of the film thickness, as seen in Figure 1a and b. This major morphology change is the formation of grass-like alumina. The morphology change from film to grass-like alumina is qualitatively seen in the SEM images in Figures 1c–e. The roughening in the SEM images matches nicely with the AFM measurements, where major surface roughness starts to form in the vicinity of 50 °C, and at lower temperatures, the film has low roughness. This kind of spiky surface morphology is unique to grass-like alumina, as the flower-like structures obtained on porous sol–gel alumina using the hot-water treatment result in distinctly rounder structures with significantly larger voids.[21,22,25]

The change in surface morphology has a great influence on the transmittance. This is shown in Figure 1f, which displays the spectral transmittance of the single-sided coated glass samples, which are the glass counterparts of the samples in Figure 1a, ensuring identical processing. Figure 1f demonstrates that below 50 °C, all the treatments in water are detrimental to the transmittance. This can be understood by the fact that the initial 28 nm-thick alumina layer has a refractive index ($n$ = 1.64) higher than that of the glass, causing less light to pass due to increased Fresnel reflection. When nearing 50 °C, the DIW causes some roughening of the surface, as indicated in Figure 1b, which causes even less light to pass due to scattering from the well separated alumina "grasslets" (Figure 1d). This roughening induces porosity, which lowers the refractive index, seen in Figure 1a. The DIW treatment at 48.2 °C is enough to cause sufficient nanoscale roughening so that the transmittance starts to increase. Above 50 °C, the nanoscale roughness is high enough to dramatically increase the spectral transmittance. The highest transmittance samples have DIW temperatures higher than 60 °C. According to the ellipsometry, these correspond to AR coatings with refractive indices of approximately $n$ = 1.20. This is extremely close to the ideal refractive index of 1.22, and it is therefore not surprising that these samples show the highest transmittance. It should be noted, however, that the ellipsometer assumes a uniform coating and can not handle a graded profile. Therefore, the values for the refractive indices and thicknesses in Figure 1a are approximate.

Figure 2 displays the spectral transmittance of double-sided coated glass samples at normal incidence. It is clear that high broadband transmittance was achieved, as all the presented samples have transmittance higher than 97% on the whole measurement range. The 90 °C sample is the best with average transmittance of 99.0% between 350 and 800 nm and peak transmittance of 99.5% at 500 nm. Furthermore, the coatings exhibit extreme omnidirectionality, as shown in Figure 3. In

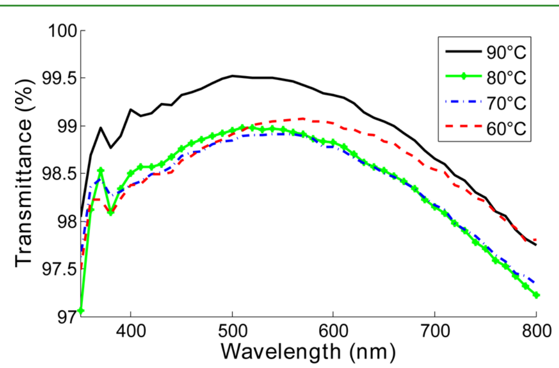


**Figure 2.** Transmission spectra of double-sided coated DIW treated samples at normal incidence.

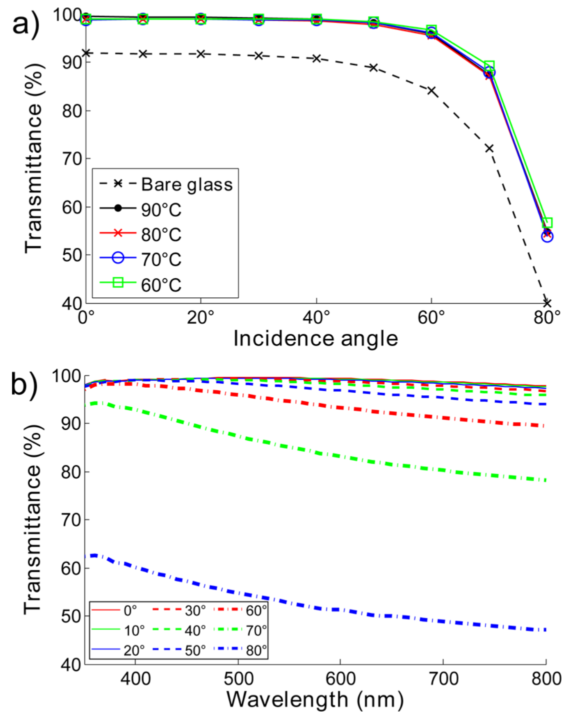


**Figure 3.** (a) Angular transmission spectra of double-sided coated DIW treated samples measured at 500 nm. The improvement of the transmittance compared to the bare glass is clear. (b) Spectral transmittance from 0–80° angles of incidence for double-sided coated glass sample treated at 90 °C.

Figure 3a, the transmittances of the double-sided grass-like alumina coated glass samples at 60° angle of incidence are all over 95%, which is significantly higher than the 91.9% for bare glass at normal incidence. Additionally, at the angle of incidence of 80° the transmittance of the coated glass slides is still roughly 16 percentage points higher than that of bare glass, further demonstrating extreme omnidirectionality. Figure 3b shows the spectral transmittance of the 90 °C sample at 0–80° angles of incidence. From Figure 3b, it is clear that broadband and omnidirectional characteristics are obtained. Below a 30° angle of incidence, the spectral transmittances are roughly the same, and the effect of the incidence angle dominates only at near glancing incidence angles. The mean spectral transmittances are 94.0% at 60°, 85.0% at 70°, and 53.1% at 80° angles of incidence, respectively.

Figure 4a shows the SEM cross section and simulated refractive index profile of the grass-like alumina treated at 90 °C DIW. The SEM image in Figure 4a shows a coating (approximately 200 nm) somewhat thicker than that in Figure 1a (125 nm using ellipsometry), and the authors consider the SEM thickness value to be more reliable, as the ellipsometer assumes a uniform coating. The simulation was done by fitting a transfer-matrix method calculation to the transmittance measurement of the double-sided coated glass sample treated at 90 °C and varying the layer refractive indices. This is a known method; other research groups have used commercial software to fit a refractive index profile to transmittance with good results,[31] but our custom-built simulation was sufficient. The simulation assumed 200 nm-thick AR coating layers


DOI: 10.1021/acsami.7b01733
ACS Appl. Mater. Interfaces 2017, 9, 15038–15043

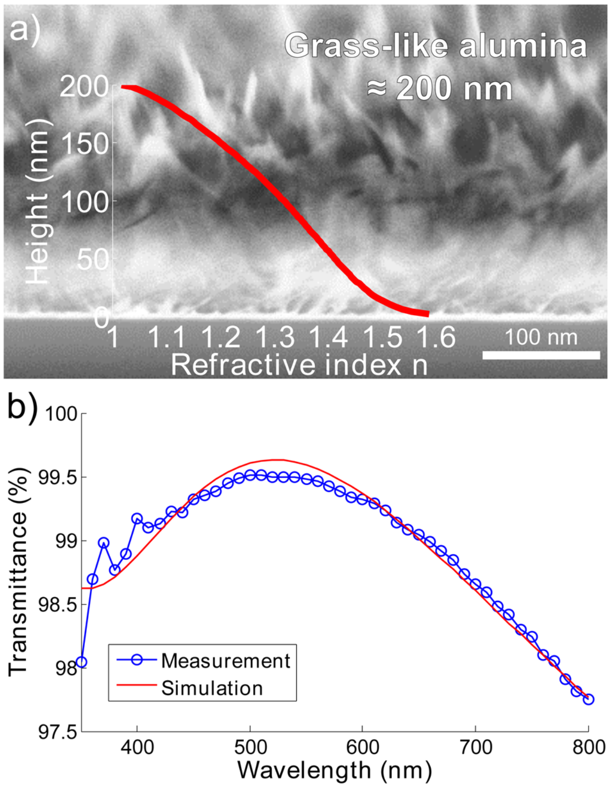


**Figure 4.** (a) Cross-sectional SEM image (imaging angle 3.4°) from grass-like alumina (90 °C DIW) with simulated refractive index profile. The charging of the alumina, which has high resistance, is clearly seen in the SEM image. (b) Spectral transmittance of double-sided coated 90 °C DIW treated sample from Figure 2 (circles) and simulated spectral transmittance (solid line).

(inferred from the SEM image) and was discretized to 1 nm layers, and the coherence length of the incident light is such that interference effects occur only in the thin coatings on the surfaces and not in the relatively thick 1 mm bulk glass (reasonable for nonlaser sources[32]). Figure 4b shows the measured and simulated transmittances. The curve with circles is the measured transmittance, and the solid curve is the simulation. The simulation matches the transmittance curve well at wavelengths over 600 nm, and below 600 nm, the match is only fair. Nevertheless, the total fit to data seems to be adequate as the normalized RMS error is only 0.0013. In addition, the calculated refractive index profile in Figure 4a is qualitatively reasonable, as the top of the grass-like alumina is clearly less dense (see Figures 1c–e and Figure 4a), and the bottom layers approach $n$ = 1.6, which shows that the bottommost layers of ALD alumina are less affected as the untreated alumina had $n$ = 1.64. As the simulation matches the results well quantitatively, and the qualitative match is good, we conclude that the actual refractive index profile should roughly match our calculations.

The authors believe that, although the long-term instability of ALD alumina is established in heated water,[17,19] the grass-like alumina coatings are stable in ambient conditions. The samples were kept in ambient (office) conditions for multiple weeks without observable changes. Moreover, there have been long-term studies[33] with similar ALD growth parameters resulting in alumina coatings that are stable in moist, warm air. Annealing the grass-like alumina films in a high temperature under nitrogen atmosphere is a proven method to make ALD alumina films water resistant.[19] Therefore, if grass-like alumina is used for prolonged periods in outdoor conditions with rain or in underwater applications, annealing could provide the needed environmental protection without significantly degrading the excellent AR properties.

As the initial alumina layer for grass-like alumina is deposited with ALD, surfaces with extreme topography can be coated. Figure 5a shows a cross-section SEM image of a black silicon surface; Figure 5b displays the same surface with 28 nm of ALD alumina, and in Figure 5c, the alumina has been DIW treated to form grass-like alumina. The arrow in Figure 5c points to one of the conformally coated valleys on the black silicon surface. Some parts of the coating have been ripped off close to the edge due to the silicon sample being cleaved, but the adhesion of the coating seems to be adequate as the cleaving process is rather dramatic. Figure 5c demonstrates that the grass-like alumina process can be used on surfaces other than glass and

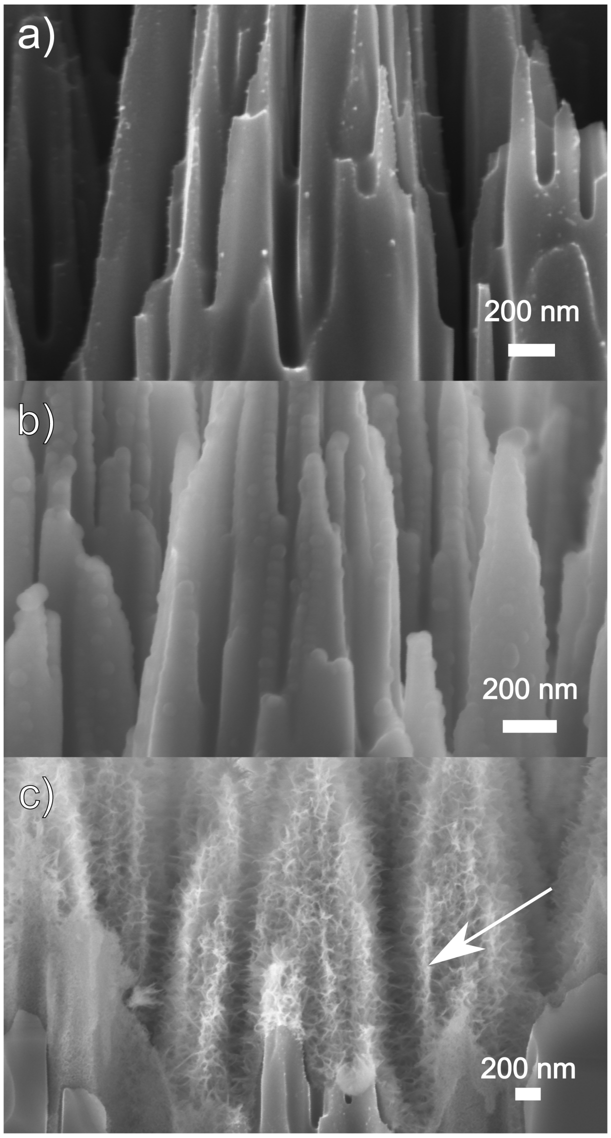


**Figure 5.** Cross section SEM images of a cleaved black silicon surface. (a) Black silicon surface without coatings. (b) Black silicon surface with conformal ALD alumina coating. (c) Black silicon surface with the same ALD alumina after DIW treatment. The arrow points to one of the conformally coated valleys.



DOI: 10.1021/acsami.7b01733
ACS Appl. Mater. Interfaces 2017, 9, 15038–15043

on surfaces with extreme topography. Similar conformality is difficult to achieve with spin-coating, dip-coating, physical vapor deposition, or glancing angle deposition, and this is the first instance of a conformal nanoporous AR coating made from alumina. Optical components with less extreme surfaces such as axicons, free-form optical components, or Fresnel lenses should be coatable with the demonstrated method. The gradient-index profile may vary when changing from planar surfaces (like the coated glass slides discussed before), but a clear gradient index still remains, as seen from Figure 5c.

The grass-like alumina coatings may have uses other than AR coatings. The spiky structure might be used with metal as a surface-enhanced Raman spectroscopy substrate, or the bare layer may be used as a cell cultivation substrate. Nanoporous filters and novel etch masks for silicon are also possible.

## 4. CONCLUSIONS

In conclusion, we demonstrated a new type of AR coating based on grass-like alumina that has high broadband transmission and excellent omnidirectionality. This single layer graded-index coating is simple to fabricate using ALD alumina and heated DIW and can be used in batch processing, thus fabricating potentially thousands of optical components in parallel, even on surfaces with extreme topography, as demonstrated on black silicon.

## AUTHOR INFORMATION

### Corresponding Author

*E-mail: christoffer.kauppinen@aalto.fi.

### ORCID

Christoffer Kauppinen: 0000-0002-2850-2702

### Author Contributions

‡C.K. and K.I. contributed equally to this work.

### Notes

The authors declare the following competing financial interest(s): Patent pending in Finland.

## ACKNOWLEDGMENTS

The authors thank the financial support of the Aalto ELEC Doctoral School of Aalto University. The nanotechnology research infrastructure in Micronova (Aalto Nanofab) enabled this work to be done. The authors thank Dr. Alexander Pyymaki Perros for fruitful discussions about ALD and Dr. Farshid Manoocheri for discussions about spectrophotometry.

## REFERENCES

(1) Clapham, P.; Hutley, M. Reduction of Lens Reflexion by the ”Moth Eye” Principle. *Nature* **1973**, *244*, 281−282.

(2) Yoldas, B. E. Investigations of Porous Oxides as an Antireflective Coating for Glass Surfaces. *Appl. Opt.* **1980**, *19*, 1425−1429.

(3) Li, X.; Gao, J.; Xue, L.; Han, Y. Porous Polymer Films with Gradient-Refractive-Index Structure for Broadband and Omnidirectional Antireflection Coatings. *Adv. Funct. Mater.* **2010**, *20*, 259−265.

(4) Chhajed, S.; Poxson, D. J.; Yan, X.; Cho, J.; Schubert, E. F.; Welser, R. E.; Sood, A. K.; Kim, J. K. Nanostructured Multilayer Tailored-Refractive-Index Antireflection Coating for Glass with Broadband and Omnidirectional Characteristics. *Appl. Phys. Express* **2011**, *4*, 052503.

(5) Poxson, D. J.; Schubert, M. F.; Mont, F. W.; Schubert, E.; Kim, J. K. Broadband Omnidirectional Antireflection Coatings Optimized by Genetic Algorithm. *Opt. Lett.* **2009**, *34*, 728−730.

(6) Chhajed, S.; Schubert, M. F.; Kim, J. K.; Schubert, E. F. Nanostructured Multilayer Graded-Index Antireflection Coating for Si Solar Sells with Broadband and Omnidirectional Characteristics. *Appl. Phys. Lett.* **2008**, *93*, 251108.

(7) Chen, J.; Wang, B.; Yang, Y.; Shi, Y.; Xu, G.; Cui, P. Porous Anodic Alumina with Low Refractive Index for Broadband Graded-Index Antireflection Coatings. *Appl. Opt.* **2012**, *51*, 6839−6843.

(8) Kennedy, S. R.; Brett, M. J. Porous Broadband Antireflection Coating by Glancing Angle Deposition. *Appl. Opt.* **2003**, *42*, 4573−4579.

(9) Jiang, H.; Yu, K.; Wang, Y. Antireflective Structures via Spin Casting of Polymer Latex. *Opt. Lett.* **2007**, *32*, 575−577.

(10) Xi, J.-Q.; Schubert, M. F.; Kim, J. K.; Schubert, E. F.; Chen, M.; Lin, S.-Y.; Liu, W.; Smart, J. A. Optical Thin-Film Materials with Low Refractive Index for Broadband Elimination of Fresnel Reflection. *Nat. Photonics* **2007**, *1*, 176−179.

(11) Poxson, D. J.; Mont, F. W.; Schubert, M. F.; Kim, J. K.; Schubert, E. F. Quantification of Porosity and Deposition Rate of Nanoporous Films Grown by Oblique-angle Deposition. *Appl. Phys. Lett.* **2008**, *93*, 101914.

(12) Rayleigh, L. On Reflection of Vibrations at the Confines of Two Media Between which the Transition is Gradual. *Proc. London Math. Soc.* **1879**, *1*, 51−56.

(13) Southwell, W. H. Gradient-Index Antireflection Coatings. *Opt. Lett.* **1983**, *8*, 584−586.

(14) Thekkekara, L.; Achanta, V. G.; Gupta, S. D. Optical Reflectionless Potentials for Broadband, Omnidirectional Antireflection. *Opt. Express* **2014**, *22*, 17382−17386.

(15) Patra, A.; Ravishankar, A. P.; Nagarajan, A.; Maurya, S.; Achanta, V. G. Quasiperiodic Air Hole Arrays for Broadband and Omnidirectional Suppression of Reflection. *J. Appl. Phys.* **2016**, *119*, 113107.

(16) Puurunen, R. L.; Saarilahti, J.; Kattelus, H. Implementing ALD Layers in MEMS Processing. *ECS Trans.* **2007**, *11*, 3−14.

(17) Abdulagatov, A. I.; Yan, Y.; Cooper, J. R.; Zhang, Y.; Gibbs, Z. M.; Cavanagh, A. S.; Yang, R. G.; Lee, Y. C.; George, S. M. Al2O3 and TiO2 Atomic Layer Deposition on Copper for Water Corrosion Resistance. *ACS Appl. Mater. Interfaces* **2011**, *3*, 4593−4601. PMID: 22032254.

(18) Kim, L. H.; Kim, K.; Park, S.; Jeong, Y. J.; Kim, H.; Chung, D. S.; Kim, S. H.; Park, C. E. Al2O3/TiO2 Nanolaminate Thin Film Encapsulation for Organic Thin Film Transistors via Plasma-Enhanced Atomic Layer Deposition. *ACS Appl. Mater. Interfaces* **2014**, *6*, 6731−6738. PMID: 24712401.

(19) Correa, G. C.; Bao, B.; Strandwitz, N. C. Chemical Stability of Titania and Alumina Thin Films Formed by Atomic Layer Deposition. *ACS Appl. Mater. Interfaces* **2015**, *7*, 14816−14821.

(20) Chen, J.; Wang, B.; Yang, Y.; Shi, Y.; Xu, G.; Cui, P. Porous Anodic Alumina with Low Refractive Index for Broadband Graded-Index Antireflection Coatings. *Appl. Opt.* **2012**, *51*, 6839−6843.

(21) Tadanaga, K.; Katata, N.; Minami, T. Super-Water-Repellent Al2O3 Coating Films with High Transparency. *J. Am. Ceram. Soc.* **1997**, *80*, 1040−1042.

(22) Yamaguchi, N.; Tadanaga, K.; Matsuda, A.; Minami, T.; Tatsumisago, M. Anti-reflective Coatings of Flowerlike Alumina on Various Glass Substrates by the Sol−Gel Process with the Hot Water Treatment. *J. Sol-Gel Sci. Technol.* **2005**, *33*, 117−120.

(23) Yamaguchi, N.; Tadanaga, K.; Matsuda, A.; Minami, T.; Tatsumisago, M. Formation of Anti-Reflective Alumina Films on Polymer Substrates by the Sol−Gel Process with Hot Water Treatment. *Surf. Coat. Technol.* **2006**, *201*, 3653−3657.

(24) Tadanaga, K.; Yamaguchi, N.; Uraoka, Y.; Matsuda, A.; Minami, T.; Tatsumisago, M. Anti-Reflective Properties of Nano-Structured Alumina Thin Films on Poly (Methyl Methacrylate) Substrates by the Sol−Gel Process with Hot Water Treatment. *Thin Solid Films* **2008**, *516*, 4526−4529.

(25) Yamaguchi, N.; Tadanaga, K.; Matsuda, A.; Minami, T.; Tatsumisago, M. Antireflective Properties of Flowerlike Alumina Thin Films on Soda−Lime Silica Glass Substrates Prepared by the Sol−Gel Method with Hot Water Treatment. *Thin Solid Films* **2007**, *515*, 3914−3917.



DOI: 10.1021/acsami.7b01733
*ACS Appl. Mater. Interfaces* 2017, 9, 15038−15043

(26) Uhlmann, D. R.; Suratwala, T.; Davidson, K.; Boulton, J.; Teowee, G. SolŮgel Derived Coatings on Glass. *J. Non-Cryst. Solids* **1997**, *218*, 113−122.
(27) Puurunen, R. L. Surface Chemistry of Atomic Layer Deposition: A Case Study for the Trimethylaluminum/water Process. *J. Appl. Phys.* **2005**, *97*, 121301.
(28) Sainiemi, L.; Jokinen, V.; Shah, A.; Shpak, M.; Aura, S.; Suvanto, P.; Franssila, S. Non-Reflecting Silicon and Polymer Surfaces by Plasma Etching and Replication. *Adv. Mater.* **2011**, *23*, 122−126.
(29) Shah, A.; Chang, B.; Suihkonen, S.; Zhou, Q.; Lipsanen, H. Surface-Tension-Driven Self-Alignment of Microchips on Black-Silicon-based Hybrid Template in Ambient Air. *J. Microelectromech. Syst.* **2013**, *22*, 739−746.
(30) Jansen, H.; de Boer, M.; Legtenberg, R.; Elwenspoek, M. The Black Silicon Method: a Universal Method for Determining the Parameter Setting of a Fluorine-Based Reactive Ion Etcher in Deep Silicon Trench Etching with Profile Control. *J. Micromech. Microeng.* **1995**, *5*, 115.
(31) Liu, L.-Q.; Wang, X.-L.; Jing, M.; Zhang, S.-G.; Zhang, G.-Y.; Dou, S.-X.; Wang, G. Broadband and Omnidirectional, nearly Zero Reflective Photovoltaic Glass. *Adv. Mater.* **2012**, *24*, 6318−6322.
(32) Donges, A. The Coherence Length of Black-Body Radiation. *Eur. J. Phys.* **1998**, *19*, 245.
(33) Carcia, P. F.; McLean, R. S.; Hegedus, S. (Invited) ALD Moisture Barrier for Cu (InGa) Se2 Solar Cells. *ECS Trans.* **2010**, *33*, 237−243.



DOI: 10.1021/acsami.7b01733
*ACS Appl. Mater. Interfaces* 2017, 9, 15038−15043